Bulletin of the Seismological Society of America, Vol. 80, No. 5, pp. 1118–1143, October 1990

THE 25 NOVEMBER 1988 SAGUENAY, QUEBEC, EARTHQUAKE: SOURCE PARAMETERS AND THE ATTENUATION OF STRONG GROUND MOTION

BY PAUL G. SOMERVILLE, JAMES P. MCLAREN, CHANDAN K. SAIKIA, AND DONALD V. HELMBERGER

ABSTRACT

The Saguenay earthquake of 25 November 1988 occurred close to the southern margin of the Saguenay Graben in southern Quebec. It was caused by almost purely dip-slip faulting centered at a depth of 26 km with a *P* axis oriented northeast-southwest. This faulting mechanism is similar to those of the larger historical earthquakes in eastern North America, but the focal depth is substantially greater than all but one of these events. The seismic moment estimated from regional *Pnl* waves and teleseismic long-period body waves is 5×10^{24} dyne-cm., corresponding to a moment magnitude of 5.8. The source duration of the earthquake is estimated to be 1.8 sec, corresponding to a stress drop of 160 bars, which is not significantly higher than the average stress drop of 120 bars estimated from previous large earthquakes in eastern North America. In order to simultaneously match the recorded ground motion amplitudes of strong-motion acceleration, strong-motion velocity, and teleseismic short-period and long-period body waves, it is necessary to use a source function having a complex shape that implies the presence of asperities and larger local stress drops. The large set of strong-motion recordings of the Saguenay earthquake has been used to validate a procedure for estimating strong ground motion attenuation based on a simple wave propagation model. The most important feature of the recorded strong motions is that their peak amplitudes do not decay significantly with distance inside 120 km, but then decay abruptly beyond 120 km. Profiles of recorded accelerograms with absolute times indicate that at distances beyond 64 km the peak ground motions are due to strong postcritical reflections from velocity gradients in the lower crust. The principal shear-wave arrivals and the variation of their peak amplitudes with distance were reproduced in synthetic seismograms generated using a regional crustal structure model. The critical distances for the postcritical reflections were short because of the deep focal depth of the event, causing the elevation of ground motion amplitudes out to 120 km. Similar studies of earthquakes in other regions of eastern North America indicate that the strength of the postcritical reflections, and the distance ranges over which they are dominant, are controlled by the focal depth and crustal structure. Regional variations in crustal structure thus give rise to predictable regional variations in strong ground motion attenuation.

INTRODUCTION

The 25 November 1988 Saguenay earthquake is the largest earthquake to have occurred in eastern North America since the 1963 Baffin Bay earthquake and the largest earthquake to have occurred in a populated region since the 1935 Timiskaming, Quebec, earthquake. The earthquake was well recorded at regional and teleseismic distances, providing an opportunity to obtain precise estimates of its source parameters. The earthquake also produced by far the largest set of strong-motion recordings of any earthquake in eastern North America. These recordings provide an opportunity to test methods, presently based on a limited data set, for estimating strong ground motions of eastern North American earthquakes.

The Saguenay earthquake occurred within the Grenville Province (Fig. 1), close to the southern margin of the Saguenay Graben in southern Quebec and about 100 km northwest of the St. Lawrence River. The earthquake occurred at 23:46:04. GMT on 25 November 1988 at latitude 48.117, longitude 71.184, and its hypocenter was at a depth of 29 km (North *et al.*, 1989). In the following, we will show that the teleseismic body waves indicate a centroid depth of 26 km, representing the average depth of a source having finite dimensions. This depth coincides with the center of the depth range of the aftershocks occurring within the first 35 hours of the main shock. The orientation in vertical cross section of a cluster of aftershocks that lie close to the main shock hypocenter coincides with the dip of the steeply eastward-dipping plane of the focal mechanism solution, suggesting that this cluster may represent the rupture surface (North *et al.* 1989).

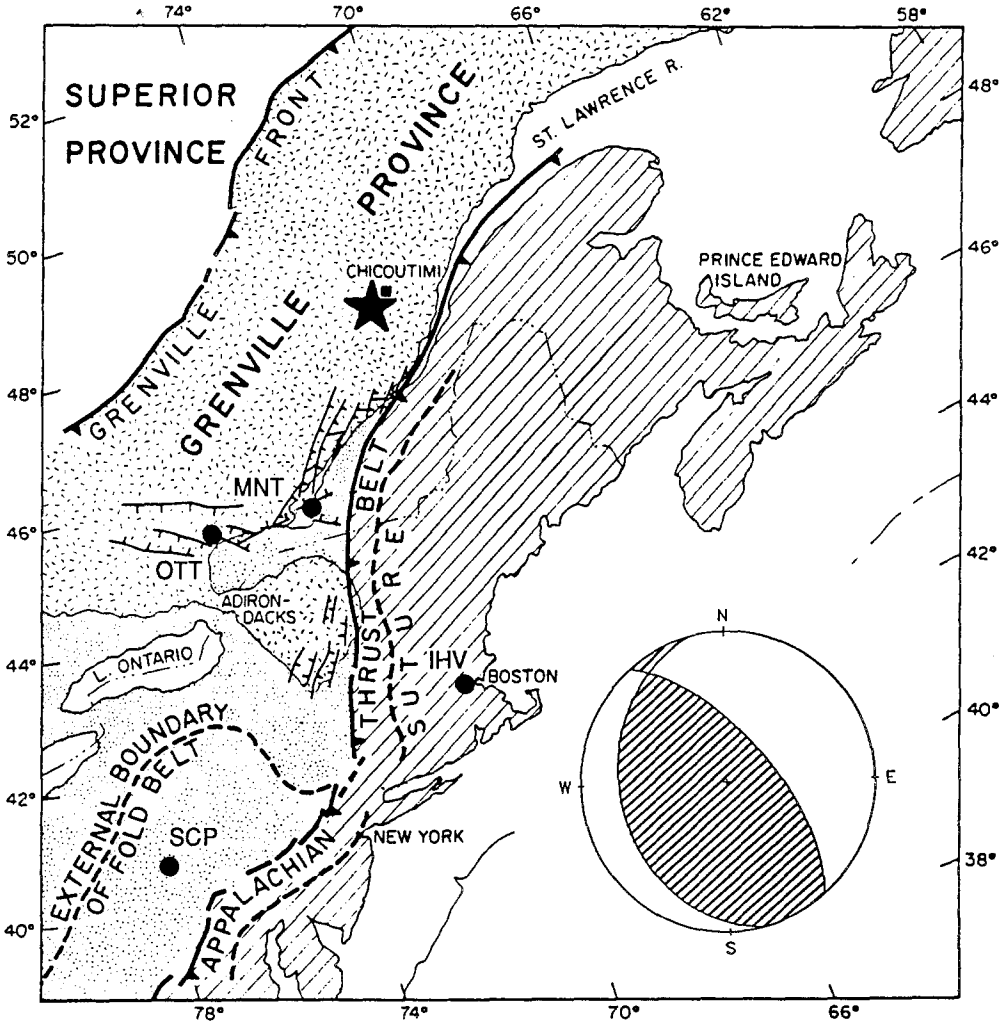

FIG. 1. Location map showing the 1988 Saguenay earthquake and its focal mechanism (lower hemisphere, compression shaded), and regional stations used for *Pnl* wave analysis. The base map showing the Superior, Grenville, and Appalachian Provinces and major tectonic features is from Hough *et al.* (1989).

Source Parameters

The estimation of source parameters of the Saguenay earthquake was performed in three stages, in which increasingly detailed aspects of the source were resolved using data having increasingly higher wave frequencies. First, we used long-period body waves to estimate the seismic moment and focal mechanism of the event, without resolving any aspect of the temporal or spatial extent of the rupture. Using these estimates of seismic moment and focal mechanism, we next analyzed teleseismic short-period body waves to estimate the overall duration of rupture of the event, without resolving any aspect of rupture complexity. Finally, using these estimates of seismic moment, focal mechanism, and source duration, we analyzed strong-motion accelerograms to derive a complex source time function of the earthquake. This source time function, shown in Figure 2, has an overall duration of 1.8 sec and contains several briefer spikes. Its derivation is described in detail below in the section entitled Strong Motion Modeling. This source-time function was used throughout all of the waveform modeling results described below; the only synthetic seismograms that are sensitive to its detailed shape are the strong-motion synthetic seismograms.

Seismic Moment and Focal Mechanism

We have used two principal data sets to simultaneously estimate the seismic moment and focal mechanism of the earthquake: *Pnl* waves (long-period regional body waves) and long-period teleseismic body waves. These two methods provide independent estimates of the source parameters, and thus allow the accuracy of the estimates to be assessed.

Pnl Waves. The term *Pnl* wave refers to the long period combination of *Pn* and *PL* waves as they propagate in the crustal wave guide to regional distances. The response for a layer over a half-space can be computed to high accuracy using generalized ray theory and very complete ray sums (Helmberger and Engen, 1980). The layer over a half-space model is sufficient for these calculations because all rays in the sum are well past critical angle and insensitive to crustal layering.

The effectiveness of using *Pnl* waves to estimate the seismic moment and focal mechanism of eastern North American earthquakes has been demonstrated in our studies of the 1963 Baffin Bay, 1986 Illinois, 1980 Kentucky, and 1982 New Brunswick earthquakes (Somerville *et al.*, 1987; Somerville, 1986). These studies showed that *Pnl* waves provide estimates of seismic moment and focal mechanism that are as accurate as those obtained from long period teleseismic body waves. In particular, seismic moment estimates derived from *Pnl* waves are less subject to uncertainty because they are longer in period and their travel paths are shorter.

The four stations used in the *Pnl* analysis are listed in Table 1 and shown in Figure 1. Unfortunately, severe microseisms greatly reduced the signal-to-noise ratio of recordings of the Canadian Network, especially those close to the Atlantic and Arctic Ocean coasts. Figure 3 compares recorded and synthetic *Pnl* waveforms and amplitudes for the preferred focal mechanism. SCP is a GDSN station, MNT and OTT are analog Canadian stations, and IHV is the digital Streckeisen instrument operated by Harvard University. Recorded and synthetic seismograms were filtered with a trapezoidal filter of 3 sec duration, since this analysis is directed toward the long-period energy. The mechanism solution satisfies the three compressional and one dilatational first motions. The waveforms at stations SCP, OTT, and SCH are relatively insensitive to changes in the rake of the mechanism solution.

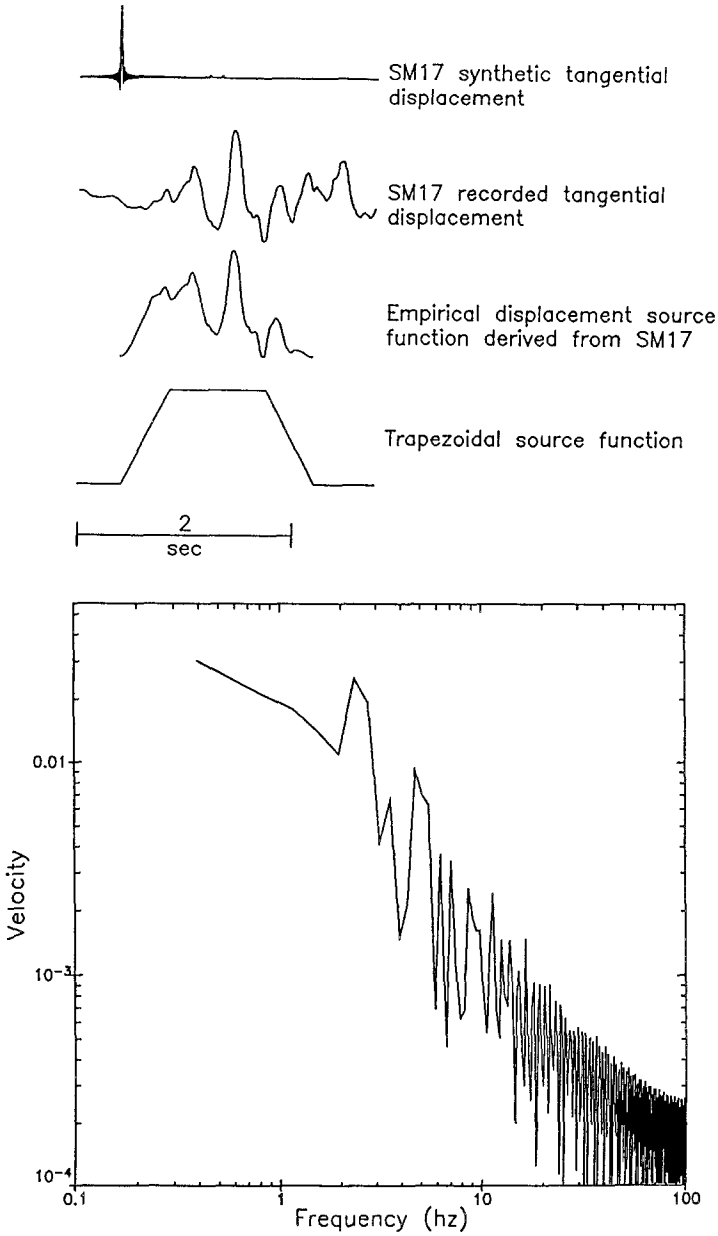

FIG. 2. Derivation of an empirical source function from the tangential S wave recorded at strong motion station SM17, and the Fourier amplitude spectrum of the empirical source function.

However, the amplitude of the first half-cycle of motion at station IHV is sensitive to the rake and favors our solution over that of North *et al.* (1989), as shown at the bottom of Figure 3. Also, the Love-to-Rayleigh wave ratio of these waves is more consistent with the preferred solution (Kanamori, personal comm., 1989). The amplitudes of the *Pnl* waves yield a seismic moment of 5.0×10^{24} dyne-cm. This estimate is identical to the estimate of 5.0×10^{24} dyne cm. obtained by modeling the surface waves recorded at IHV (Zhao and Helmberger, 1989).

TABLE 1

STATIONS USED IN *Pnl* ANALYSIS

Code	Network	Station	Distance (degrees)	Azimuth
OTT	CAND	Ottawa, Ontario	4.137	230.42
IHV	STRK	Harvard, Massachusetts	5.738	181.01
SCH	CAND	Schefferville, Quebec	7.253	20.61
SCP	WWSS	State College, Pennsylvania	8.727	215.62

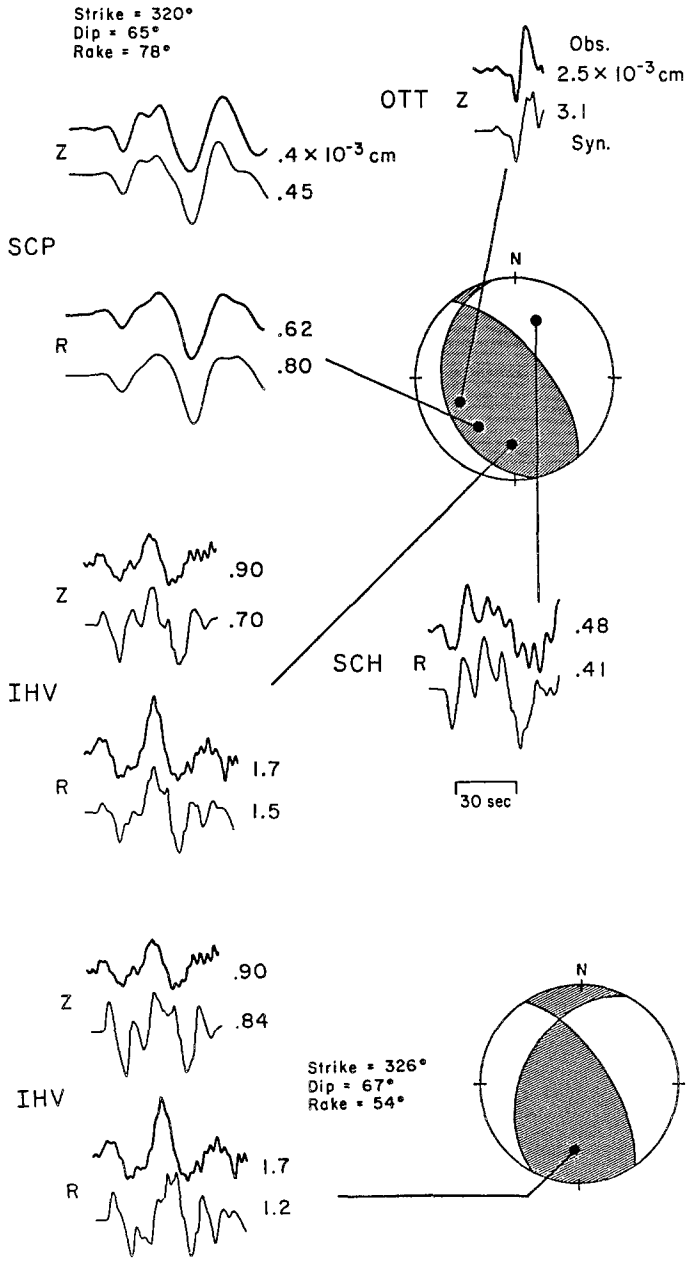

FIG. 3. Comparison of recorded and simulated *Pnl* waves for the preferred focal mechanism (*top*); a comparison at station IHV is also shown for the focal mechanism of North *et al.* (1989) (*bottom*). Amplitudes are shown in units of 10^{-3} cm, and mechanisms are lower hemisphere with compression shaded.

Teleseismic Long-Period Body Waves. The procedure of Langston and Helmberger (1975) was used to model the amplitudes and waveforms of teleseismic long-period body waves of the Saguenay earthquake. This procedure has been applied to earlier eastern North American earthquakes by Ebel *et al.* (1986). The stations used in the analysis are listed in Table 2. A source depth of 26 km was found to provide the best agreement with depth-phase times in the long-period and short-period teleseismic records. To represent the effects of anelastic absorption, we used a Futterman (1962) attenuation operator having a t^* of 0.7; the amplitudes and waveforms of synthetic long-period seismograms are not very sensitive to realistic variations in the value of t^* used.

The vertical P waves, shown in Figure 4, have nodal direct P phases at European stations, where the largest phase is pP. In western North America (DUG), the pP phase is nodal, and the largest phase is sP. The vertical, transverse, and radial components of the long-period S waves at six stations are shown in Figure 5. A notable feature of the radial motions is the presence at European stations of the phase pS, which is prominent only because the sS phase is nodal for these stations. Away from the node, the sS phase is clearly visible, for example in the tangential component recordings at MBC and DUG. These specific features of the waveforms provide strong confirmation of the focal depth and focal mechanism of the event, although they do not allow us to resolve between our preferred solution and that of North *et al.* (1989).

The seismic moment estimate from these long-period body waves is 4.3×10^{24} dyne-cm, which is not significantly different from the estimate of 5.0×10^{24} dyne-cm obtained from the *Pnl* waves. Noting that seismic moment estimates derived from *Pnl* waves are less subject to uncertainty in t^*, we adopt the value of 5.0×10^{24} dyne-cm and estimate an associated uncertainty of a factor of 1.25 based on the variability of a factor of 1.2 in the *Pnl* estimates from different stations and the variability of a factor of 1.15 between the *Pnl* and long-period teleseismic estimates. This seismic moment value corresponds to a moment magnitude of 5.8. The reported magnitudes of the Saguenay earthquake are an M_s of 5.8 (NEIS), an m_b of 5.9 (NEIS), and an m_{bLg} of 6.5 (GSC). At the end of the paper, we use synthetic seismograms to estimate an m_{bLg} of 6.4 and conclude that the measured value of 6.5 is compatible with the source and wave propagation models that we derive from other data.

Source Duration and Source Dimensions

In order to obtain a more detailed description of the earthquake source, we modeled a set of teleseismic short-period and broadband P-wave seismograms

TABLE 2

STATIONS USED IN LONG-PERIOD TELESEISMIC BODY-WAVE ANALYSIS

Code	Network	Station	Distance (degrees)	Azimuth
LUB	WWSS	Lubbock, Texas	27.162	248.95
DUG	WWSS	Dugway, Utah	30.585	270.66
MBC	CAND	Mould Bay, Canada	34.142	341.47
BOG	WWSS	Bogota, Colombia	43.403	184.19
KEV	WWSS	Kevo, Finland	48.519	27.38
KJF	WWSS	Kajaani, Finland	51.534	33.52
NUR	WWSS	Nurmijarvi, Finland	52.315	38.46
IST	WWSS	Istanbul, Turkey	66.670	54.18

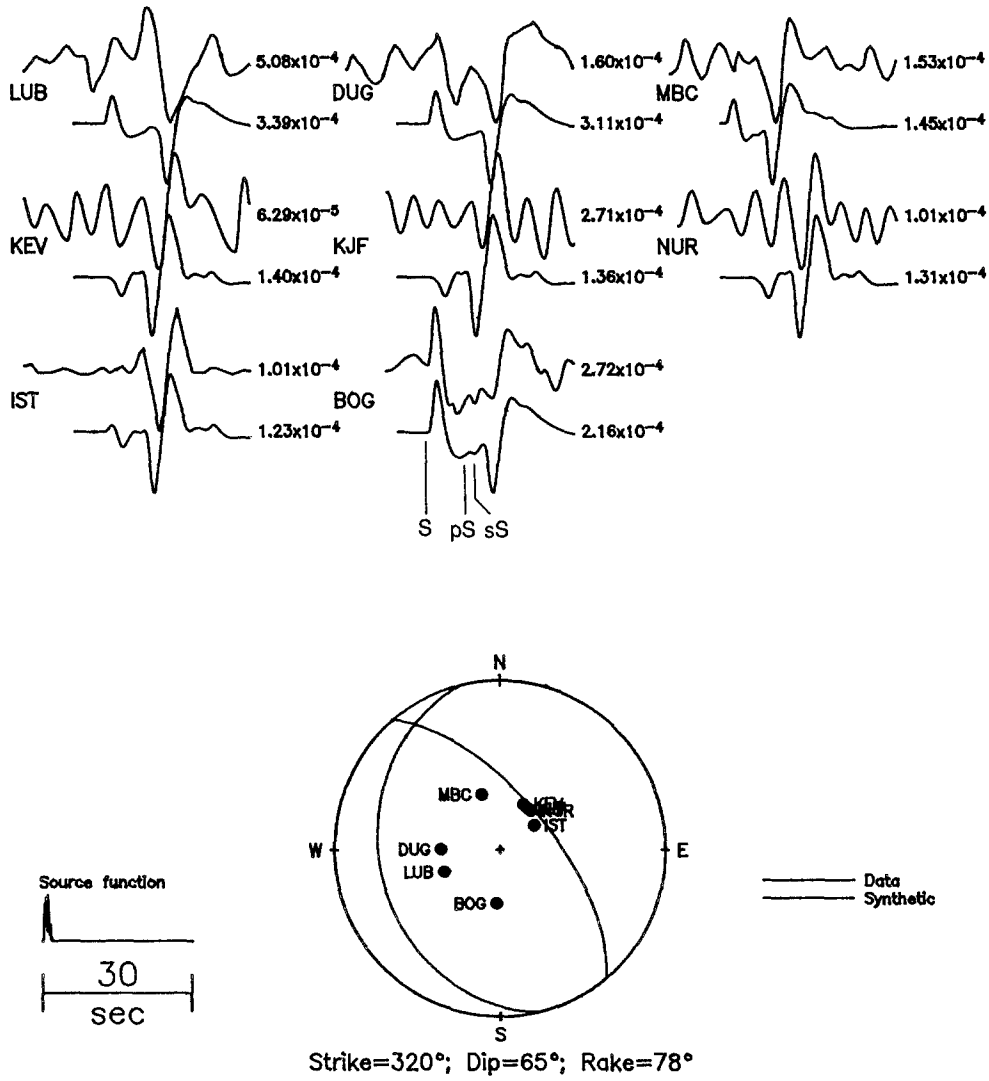

FIG. 4. Comparison of recorded (upper trace) and synthetic (lower trace) long-period teleseismic *P* waves of the Saguenay earthquake, with amplitudes shown in cm.

recorded at the stations listed in Table 3. This provided an estimate of the overall duration of the source but did not resolve details of the source function.

Figure 6 shows seismograms recorded digitally on instruments having a variety of instrument responses, together with synthetic seismograms. The seismograms shown in Figure 7 were recorded in analog form on WWSSN or Caltech stations. We observe several features common to both the recorded and synthetic seismograms. Most stations in the Americas have large *P* and *sP* phases and small *pP* phases. At COL, Alaska, and WMQ, China, both *P* and *pP* are large and *sP* is small. The European stations have large *pP* phases but are nodal for direct *P* and *sP*; the nodal nature of the latter phases is reflected in the large unmodeled phases in the seismograms recorded in Europe. The timing of these depth phases is consistent with a centroid source depth of 26 km.

Overall, the complex source function provides fairly good agreement in both amplitude and waveform between the recorded and synthetic seismograms using an

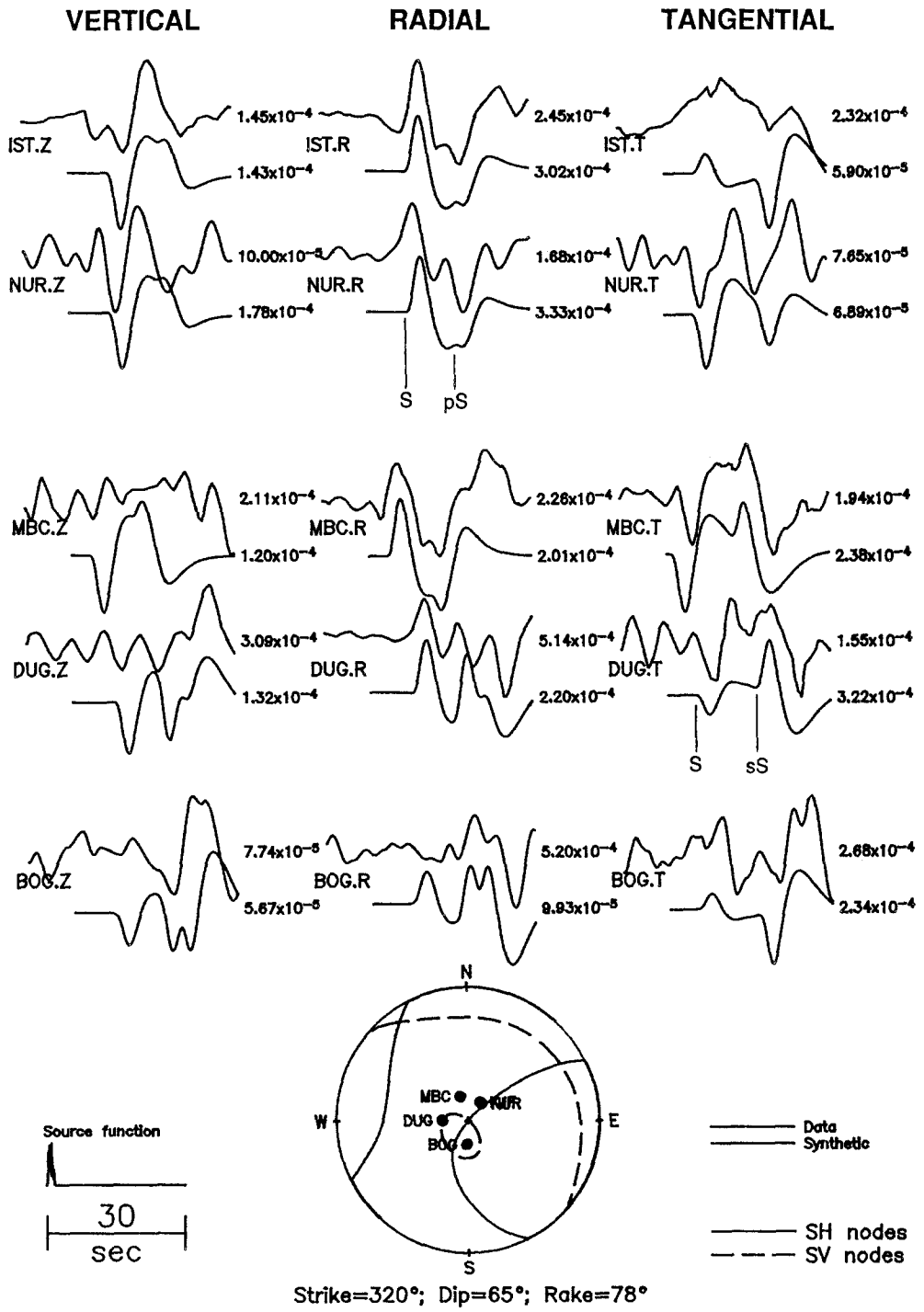

FIG. 5. Comparison of recorded (upper trace) and synthetic (lower trace) long-period teleseismic *S* waves of the Saguenay earthquake, with amplitudes shown in cm.

absorption operator with a t^* of 0.7, which is representative of measured values at short periods. An equally good fit in waveform and amplitude was obtained using the trapezoidal source function (shown in Fig. 2) having the same overall duration of 1.8 sec. We estimate the uncertainty in the duration to be a factor of 1.3, based

TABLE 3

STATIONS USED IN SHORT-PERIOD TELESEISMIC BODY-WAVE ANALYSIS

Code	Network	Station	Distance (degrees)	Azimuth
ANMO	GDSN	Albuquerque, New Mexico	29.200	256.30
LON	WWSS	Longmire, Washington	33.692	286.99
CMB	GDSN	Columbia Col, California	36.600	272.70
MWC	CIT	Mount Wilson, California	37.334	265.72
COL	WWSS	College Outpost, Alaska	42.300	322.20
BOG	WWSS	Bogota, Colombia	43.403	184.19
TOL	WWSS	Toledo, Spain	47.592	73.80
GRFO	GDSN	Grafenberg, Germany	51.300	55.20
ZOBO	GDSN	Zongo (La Paz), Bolivia	52.315	183.30
NUR	WWSS	Nurmijarvi, Finland	64.400	38.46
IST	WWSS	Istanbul, Turkey	66.670	54.18
PEL	WWSS	Peldehue, Chile	80.893	179.58
WMQ	GDSN	Urumqi, China	86.200	15.10

on the variability in duration at different stations of a factor of 1.2 for an assumed t^* of 0.7, and the variability of a factor of 1.2 in duration due to uncertainty in the value of t^*.

Assuming that the source duration reflects the duration of rupture propagation (at 0.8 times the shear-wave velocity) and of slip on a circular fault (Cohn *et al.*, 1982), this source duration corresponds to a fault radius of 2.5 km and a fault area of 20 km^2. The fault dimensions derived from the source duration are significantly smaller than the overall horizontal dimensions of 40 km of the aftershock sequence (North *et al.*, 1989). The source duration estimated here is consistent with these authors' suggestion that the main shock ruptured a region that is smaller than the aftershock zone. The centroid depth of 26 km estimated from teleseismic depth phases coincides with the center of the depth range of aftershocks occurring within the first 35 hours of the main shock (North *et al.*, 1989). The fault radius of 2.5 km and centroid depth of 26 km are consistent with the rupture having propagated upward from a hypocentral depth of 29 km on the steeply eastward dipping nodal plane. We looked for evidence of source finiteness in the short-period body waves using fault planes having areas of 20 km^2, but did not find a finite source model that provided a better fit to the data than the point source model we have described.

Comparison with other Eastern North American Earthquakes

The mechanism of the Saguenay earthquake is nearly pure thrust with a P axis oriented east-northeast, consistent with that of the larger earthquakes in the northeastern United States and southeastern Canada (Ebel *et al.* 1986, Somerville *et al.*, 1987). The Saguenay earthquake originated at a depth of 29 km, which is greater than the depth range of 5 to 15 km that is characteristic of the larger earthquakes in eastern North America (Ebel *et al.* 1986; Somerville *et al.*, 1987). The only earthquake having a comparable depth was the 1968 Illinois earthquake, at a depth of 25 km.

The overall source duration of the earthquake of 1.8 sec, combined with a seismic moment of 5×10^{24} dyne-cm, corresponds to a stress drop of approximately 160 bars. The uncertainties of a factor of 1.25 in seismic moment and 1.3 in duration yield an uncertainty of a factor of 2.3 in stress drop. The estimate of

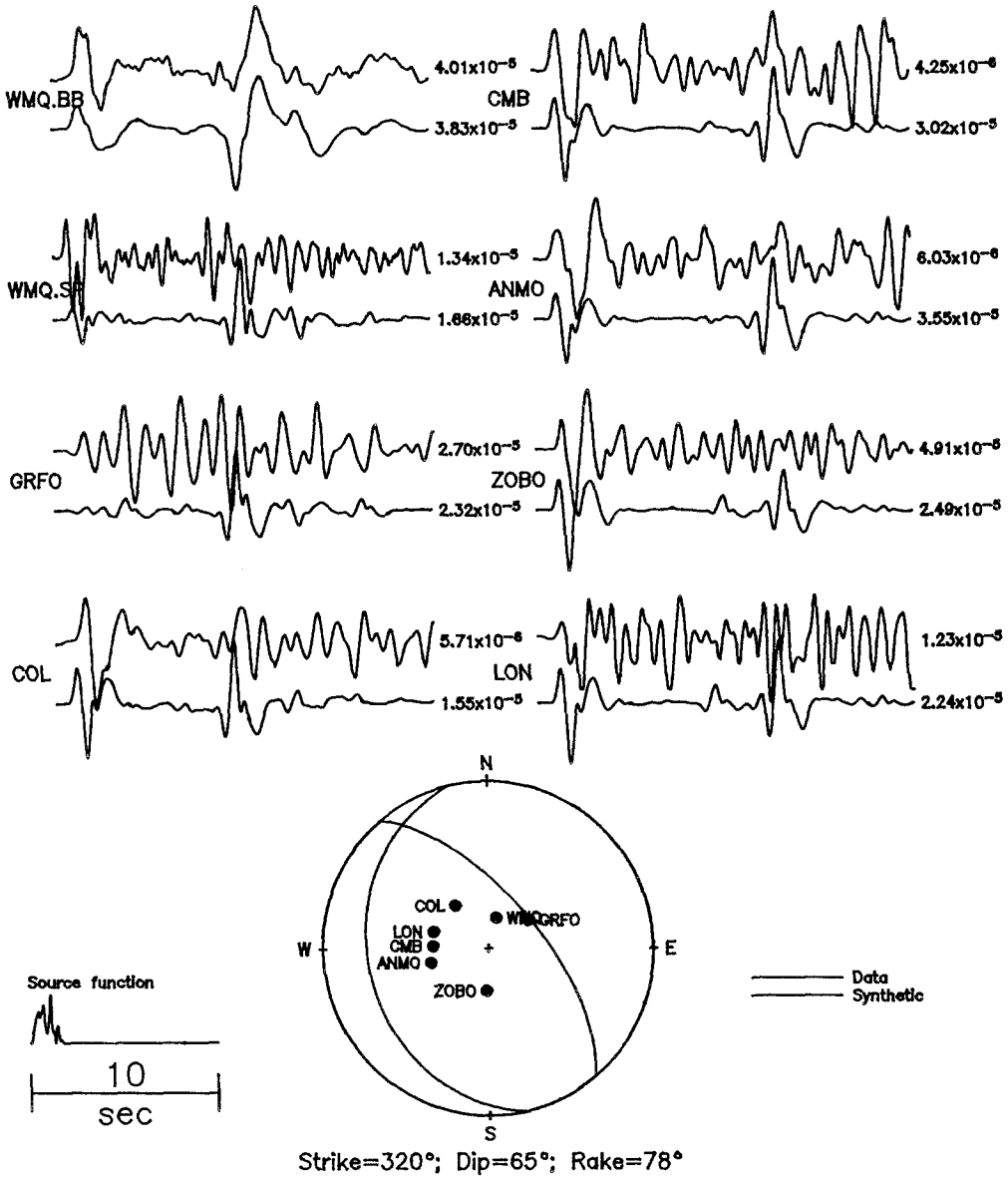

FIG. 6. Comparison of recorded (upper trace) and synthetic (lower trace) vertical GDSN short-period teleseismic *P* waves of the Saguenay earthquake, with amplitudes shown in cm.

160 bars is well within the uncertainty of a factor of 1.8 in the median value of 120 bars obtained from 13 previous eastern North American events using the same method (Somerville *et al.*, 1987). The stress drop of the Saguenay earthquake is thus compatible with those of previous events in eastern North America, as shown in Figure 8.

STRONG-MOTION MODELING

Introduction

Because of the small size of the strong-motion data base for eastern North American earthquakes, synthetic seismogram techniques have played an important

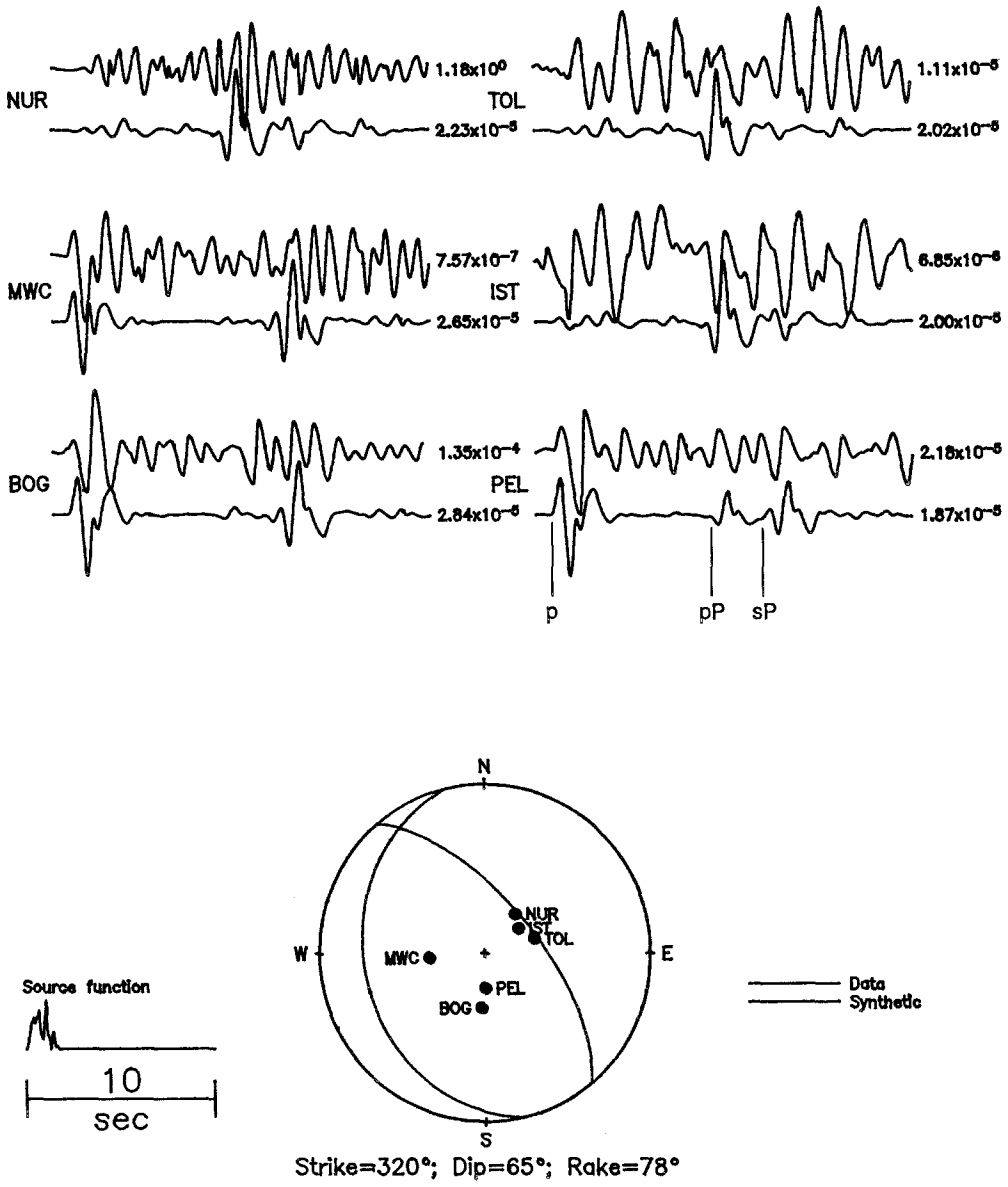

FIG. 7. Comparison of recorded (upper trace) and synthetic (lower trace) vertical WWSSN and CIT short-period teleseismic *P* waves of the Saguenay earthquake, with amplitudes shown in cm.

role in the development of ground motion attenuation relations for eastern North America in recent years. The most common approach uses random process theory (Hanks and McGuire, 1981; Boore, 1983), in which strong ground motions are modeled as segments of band-limited noise. Wave propagation effects are modeled by anelastic attenuation and by a geometrical spreading term, assumed to be $1/R$ within 100 km (corresponding to body wave spreading in a whole-space), and $1/\sqrt{R}$ beyond 100 km (corresponding to surface wave spreading in a half space). These effects produce a smooth, monotonically decreasing function of ground motion amplitude with distance (Boore and Atkinson, 1987; Toro and McGuire, 1987).

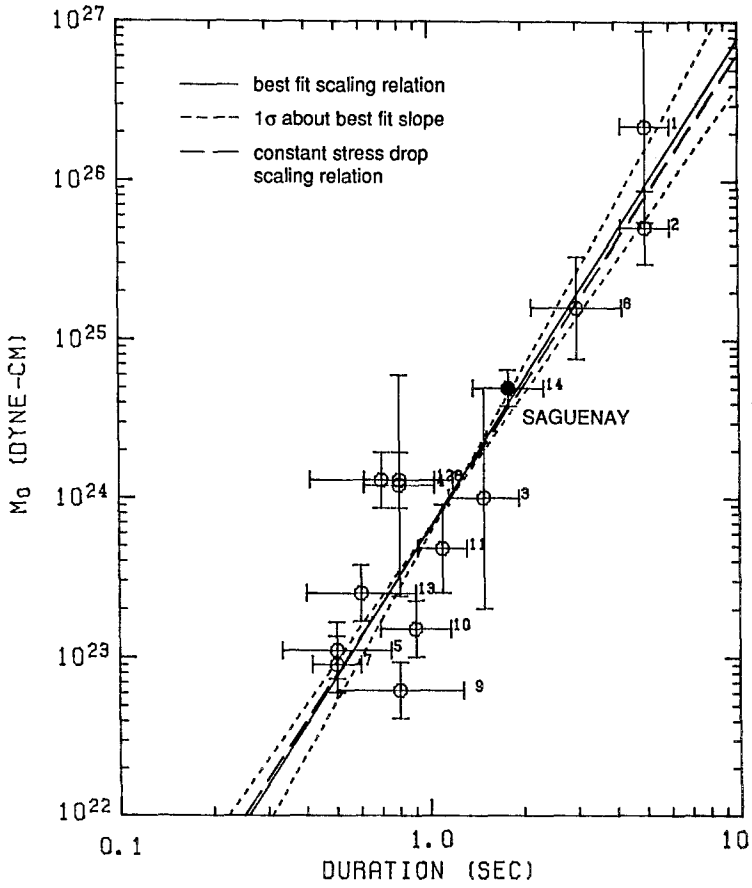

FIG. 8. Comparison of the source parameters of the Saguenay earthquake with those of other eastern North American earthquakes. The numbers refer to event numbers in Table 1 of Somerville *et al.* (1987). Modified from Somerville *et al.* (1987).

Burger *et al.* (1987) investigated the effect of wave propagation in the crustal waveguide on the shape of the ground motion attenuation curve. The principal seismic phases associated with wave propagation in a crustal waveguide are shown schematically in simplified form in Figure 9a. At close distances, peak horizontal ground motions are controlled by direct upgoing shear waves. As distance increases, the reflections of the shear wave from interfaces in the lower crust (such as those at 30 and 40 km in Fig. 9a) reach the critical angle and undergo total reflection. The strong contrast in elastic moduli at these interfaces, especially at the Moho (the base of the crust) causes these reflected phases to have large amplitudes. Using synthetic seismograms (Fig. 9b), Burger *et al.* (1987) found that peak ground motion amplitudes at distances beyond about 50 km are controlled by these postcritical reflections from velocity gradients in the lower crust (Fig. 9c). They found evidence supporting this result in empirical strong motion data (Toro and McGuire, 1987, Figs. 6 through 9) that showed a flat trend in the distance range of 60 to 150 km.

Further studies of ground motion attenuation using digital network data and strong-motion recordings in the northeastern United States and adjacent Canada (Barker *et al.*, 1988, 1989) and in Virginia and the south-central United States (Saikia *et al.*, 1989) lent support to the hypothesis that crustal structure, and

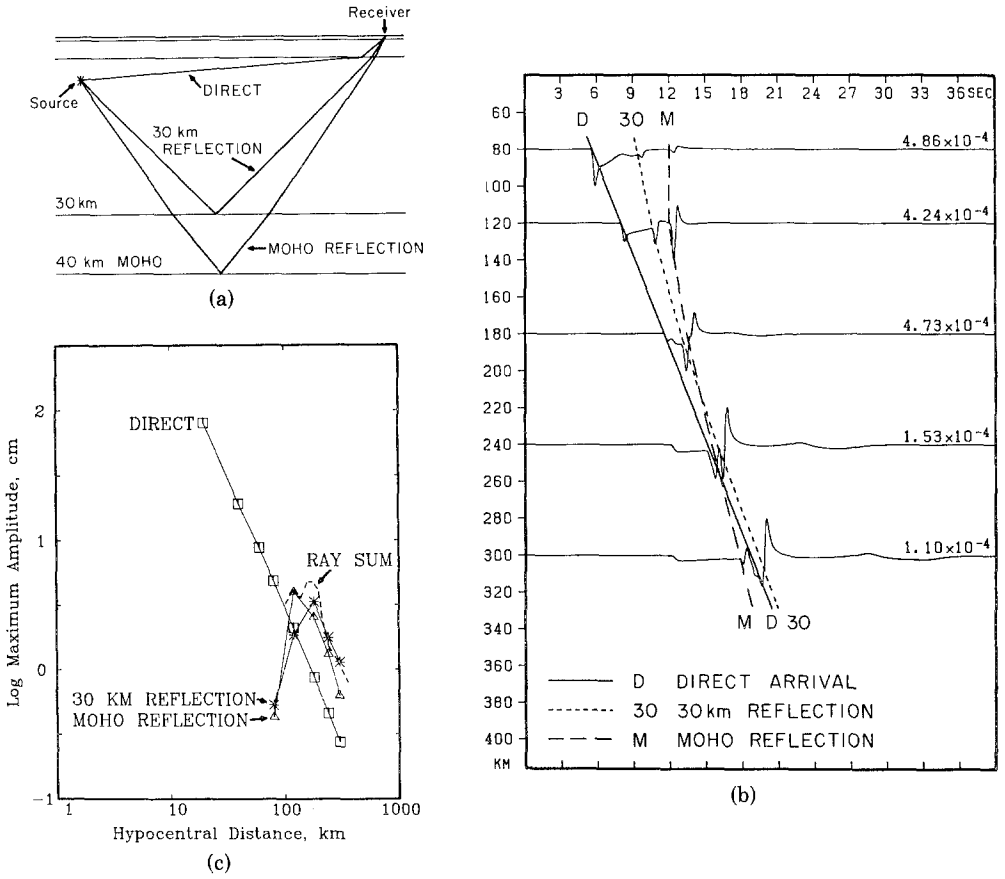

FIG. 9. (a) Simplified model of wave propagation in a layered crust; (b) synthetic displacement seismograms for the crustal model shown in (a); (c) attenuation of direct and reflected phases shown in (b). Source: Burger *et al.* (1987).

specifically, postcritical reflections from the velocity gradient in the lower crust, play an important role in determining the shape of the strong ground motion attenuation curve. Using the procedure developed by Burger *et al.* (1987) and Barker *et al.* (1988), Gariel and Jacob (1989), and Ou and Herrmann (1990) analyzed the attenuation of strong motion from the 1988 Saguenay earthquake and obtained results similar to those we present below.

Strong-Motion Recordings

The Saguenay earthquake produced by far the largest set of strong motion recordings of any earthquake in eastern North America. Our objective in analyzing these recordings is to test the suggestion of Burger *et al.* (1987) that postcritical reflections from velocity gradients in the lower crust strongly control the peak amplitudes of ground motions in the distance range of about 50 to 200 km. The locations of recording stations are shown in Figure 10; the inset shows the locations of triggered strong-motion stations within 200 km of the source, which are listed in Table 4. The main shock was recorded on analog accelerographs of the Canadian seismic network (Munro and North, 1988), on digital accelerographs of the National Center for Earthquake Engineering Research (NCEER) network (Friberg *et al.*,

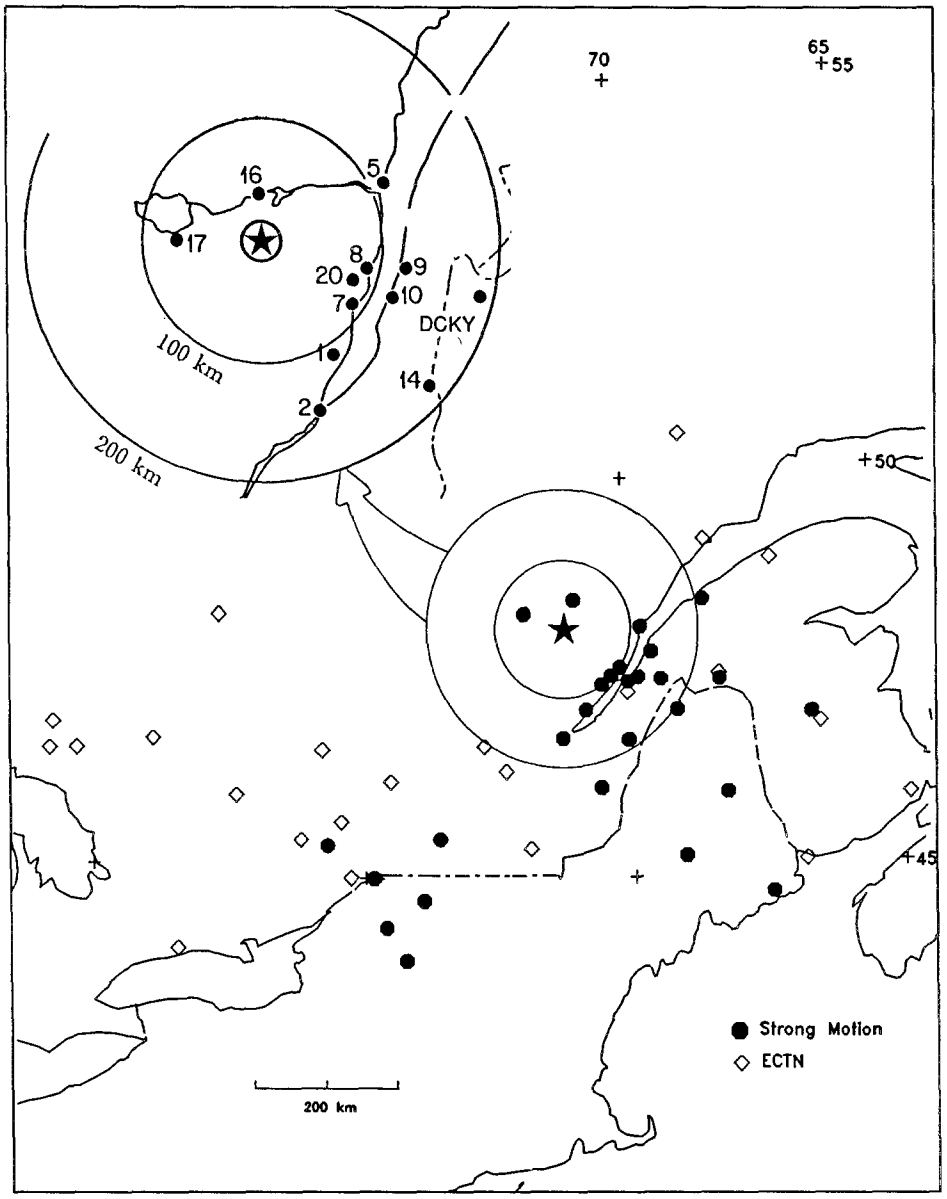

FIG. 10. Locations of strong motion and ECTN stations, and inset showing triggered strong motion stations. Modified from Munro *et al.* (1988) and Munro and North (1988).

1989), and on stations of the digital Eastern Canada Telemetered Network (Munro *et al.*, 1988), although stations of the ECTN within 300 km went off scale. All of these recordings have absolute clock times, allowing the construction of record profiles and facilitating the identification of seismic phases.

Crustal Structure Model

The 1988 Saguenay earthquake sequence occurred within the Grenville Province. The boundary between the Grenville Province and the Appalachian Province is generally described by the St. Lawrence River (Fig. 1), although the Adirondack

TABLE 4

STRONG GROUND MOTION STATIONS

Code	Station	Distance (km)	Azimuth
Eastern Canada Strong Motion Stations:			
SM16	Chicoutimi Nord, Quebec	43.41	17.00
SM17	St-Andre, Quebec	64.31	291.36
SM20	Les Eboulements, Quebec	89.96	134.21
SM07	Baie-St-Paul, Quebec	90.57	145.67
SM08	La Malbaie, Quebec	92.65	123.26
SM05	Tadoussac, Quebec	109.10	87.92
SM01	St-Ferreol, Quebec	113.42	166.23
S10	Riviere-Ouelle, Quebec	114.03	128.26
S09	St Pascal, Quebec	122.44	121.96
SM02	Quebec, Quebec	149.00	182.67
S14	Ste Lucie de Beauregard, Quebec	176.46	149.64
NCEER Strong Motion Array:			
DCKY	Dickey, Maine	198.3	125.3

Mountains which lie to the south of the St. Lawrence belong to the Grenville Province. The difference in crustal structure between these provinces has been shown to cause corresponding differences in wave propagation and ground motion attenuation characteristics (Barker *et al.*, 1989). To avoid the complexities associated with wave progagation across this province boundary, we have chosen to model the strong-motion recordings within 200 km of the source. This subset includes recording stations within the Grenville province, and stations outside the Grenville Province for which the postcritical crustal reflections occur within the Grenville Province.

Although the foreshock and largest aftershock were not recorded on strong-motion instruments, they were both recorded by the ECTN. Profiles of these recordings were used in deriving a crustal structure model for the Saguenay region because these events had simpler and briefer source functions than the main shock. The starting model was based on model 1W of Berry and Fuchs (1973); the western end of line 1 is approximately 170 km north-northeast of the Saguenay earthquake epicenter, within the Grenville Province. The final model, shown in Table 5, has a Moho depth of 43 km and a Conrad discontinuity at a depth of 33 km, which is 5 km below the hypocenter of the Saguenay earthquake. The fit of the travel-time curves of this structure model to the main-shock strong-motion recordings is shown in Figures 11 through 14, and described below.

Wave Propagation Model

Wave propagation between the source and the recording stations was represented by theoretical Green's functions computed for this structure model using the frequency-wavenumber method for a point source at a depth of 28 km. (This depth is equivalent to the hypocentral depth of 29 km in the crustal structure model used by North *et al.*, 1989). The Nyquist frequency for these computations was 50 Hz. The hypocentral depth of 28 km was used rather than centroid depth of 26 km in order to match the arrival times of seismic phases. The effects of absorption and scattering between the source and the recording station were not included in the Green's functions, since they are present in the empirical source function derived from the strong-motion recordings at station SM17 as described below. These

TABLE 5

CRUSTAL STRUCTURE MODEL FOR THE SAGUENAY REGION

Compressional Wave Velocity (km/sec)	Shear-Wave Velocity (km/sec)	Density (gm/cc)	Thickness (km)
4.5	2.6	2.30	1.44
5.5	3.4	2.50	6.0
6.1	3.5	2.67	12.0
6.6	3.7	2.85	14.0
7.0	4.0	3.02	10.0
8.2	4.7	3.35	

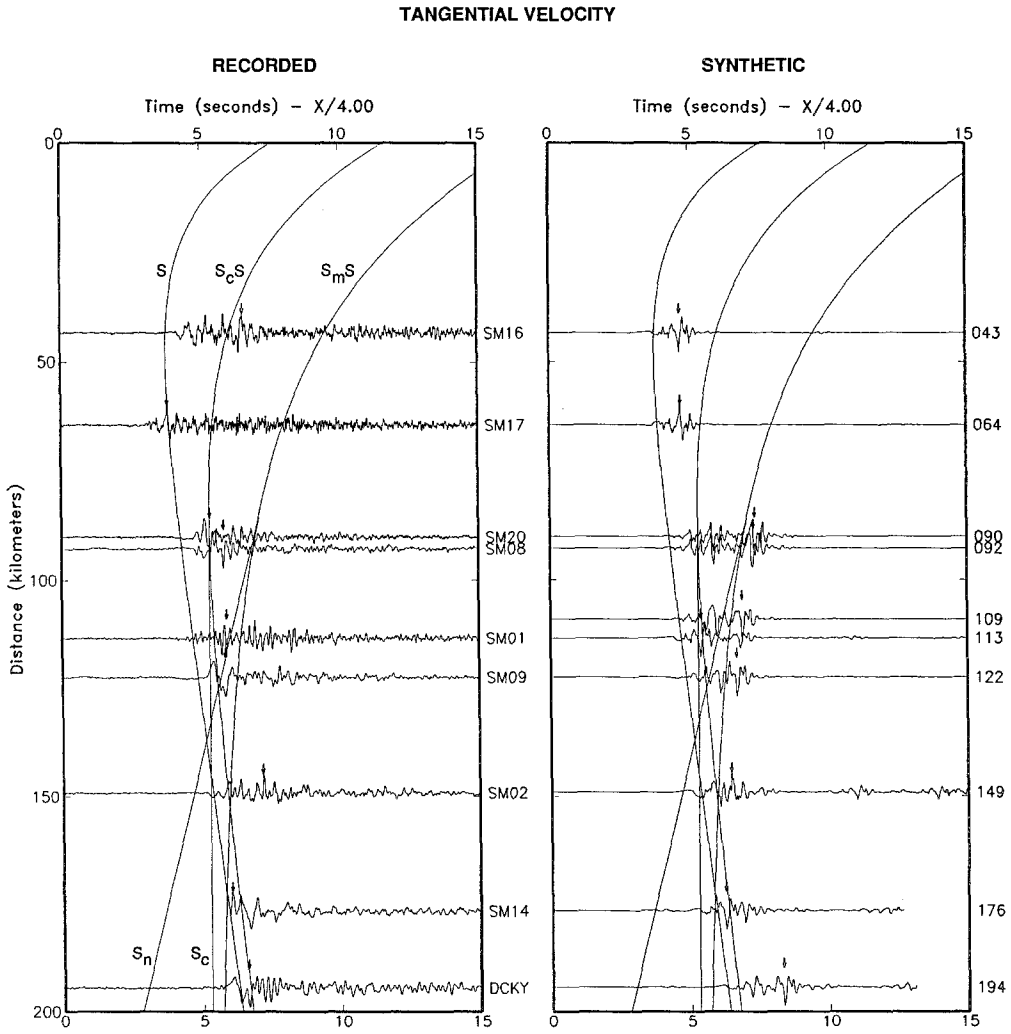

FIG. 11. Profiles of recorded (*left*) and synthetic (*right*) tangential velocity of the Sàguenay earthquake. Seismograms are individually normalized. Station numbers refer to the inset in Figure 10.

effects were assumed to be an adequate representation of attenuation and scattering along the path to the other strong-motion stations, since it appears that within distances of 200 km, most of the attenuation occurs within the shallow crust beneath the recording station (e.g., Hough and Anderson, 1988).

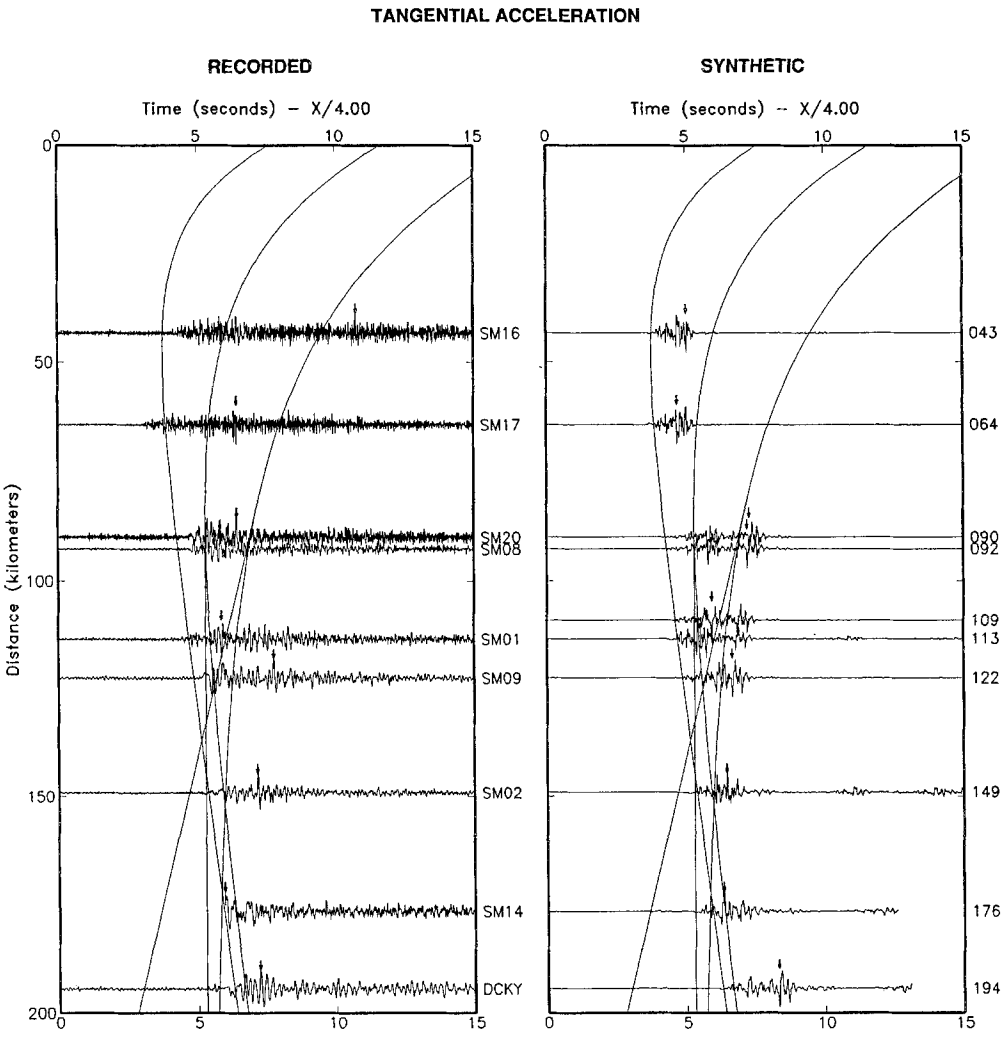

FIG. 12. Profiles of recorded (*left*) and synthetic (*right*) tangential acceleration of the Saguenay earthquake.

Source-Time Function

The analysis of the teleseismic short-period seismograms described above yielded an estimate of 1.8 sec for the overall source duration of the event. To estimate the detailed character of the source, we examined strong motion recordings within several source depths of the event. These recordings confirmed the teleseismic source duration estimate. The tangential component Green's function calculated at strong-motion station SM17, located at an epicentral distance of 64 km from the source, is shown in Figure 2. The simplicity of this Green's function, consisting of just the direct S wave, suggests that the strong-motion displacement at this station (shown below the Green's function) is due mainly to source effects. The duration of the source as seen in this record is compatible with the duration of 1.8 sec estimated teleseismically. Accordingly, a 1.8-sec-long segment of this recording was chosen to represent the source function of the earthquake. A source function was estimated by constraining the displacement seismogram to have positive values and

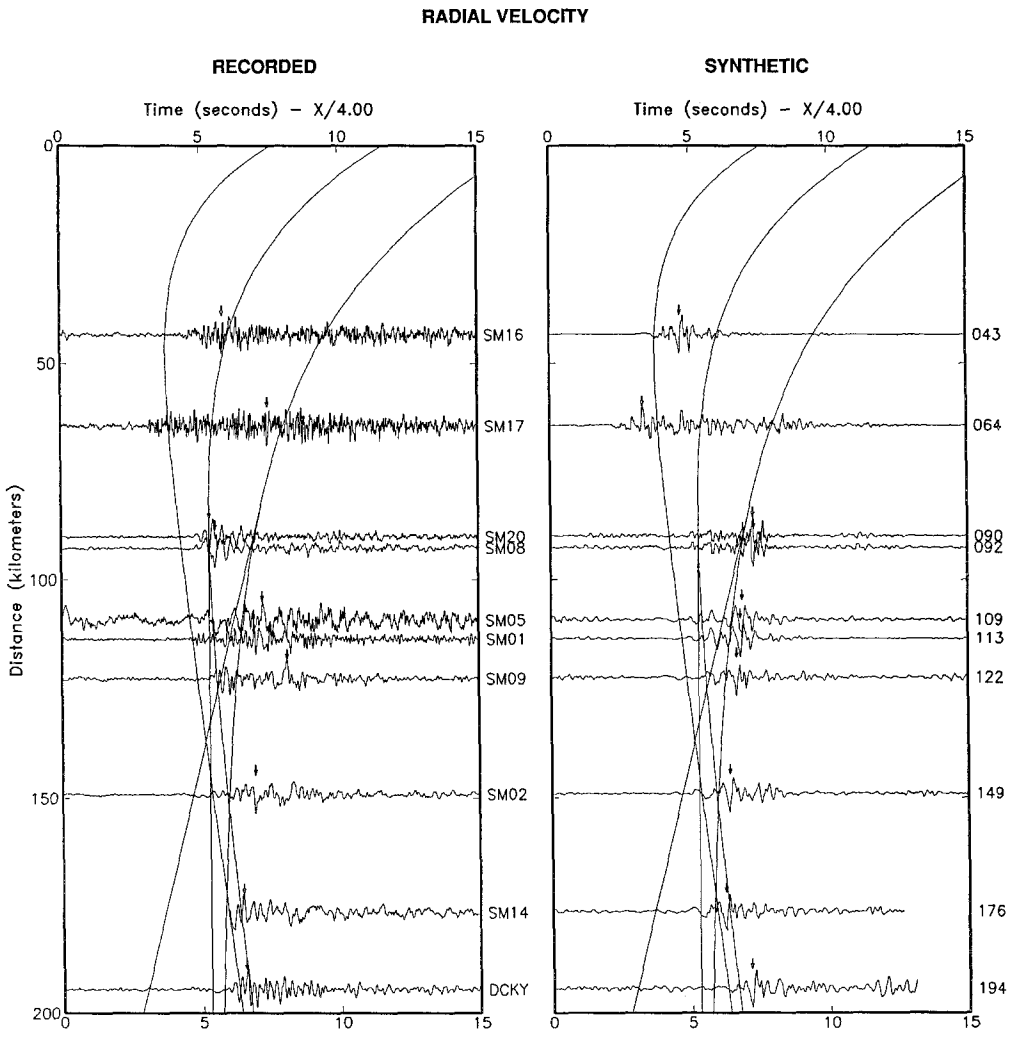

FIG. 13. Profiles of recorded (*left*) and synthetic (*right*) radial velocity of the Saguenay earthquake.

normalizing its area to represent unit seismic moment. The irregularity in the shape of this source function is used as an empirical representation of source complexity. To investigate the sensitivity of teleseismic and strong-motion synthetic seismograms to the selection of this source function, we also used a source function derived from the strong motion recording at station SM16 at an epicentral distance of 46 km. It produced results that were not significantly different from those obtained using SM17.

Modeling of Strong-Motion Recordings

In order to simultaneously match the recorded amplitudes of strong motion acceleration, strong motion velocity, and teleseismic short-period and long-period body waves, it was necessary to use a source function having the high frequency complexity of this empirical source function. While the trapezoidal source function shown in Figure 2 or a Gaussian-shaped source function provide adequate agreement with the teleseismic data, these source functions underpredict the amplitudes of the strong ground motions.

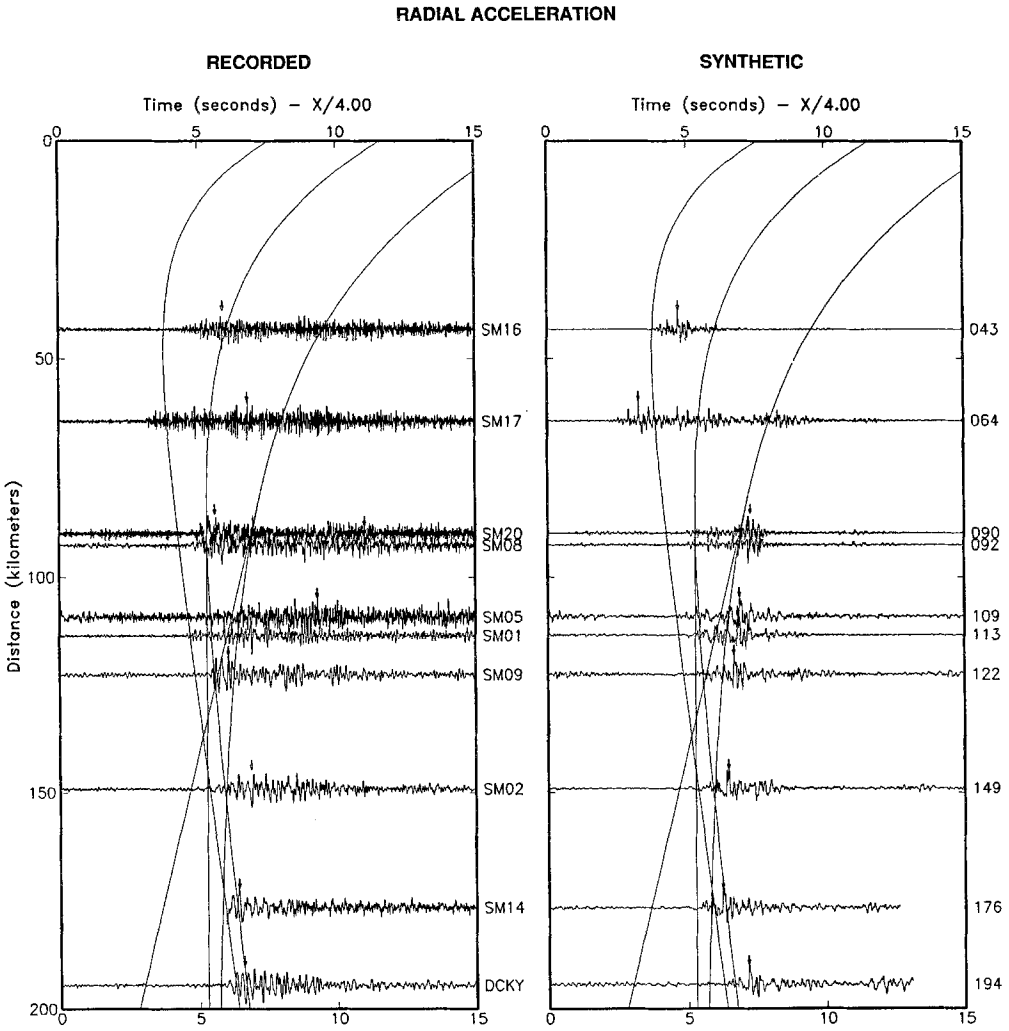

FIG. 14. Profiles of recorded (*left*) and synthetic (*right*) radial acceleration of the Saguenay earthquake.

Synthetic acceleration and velocity seismograms for the radial and tangential components of motion were computed at the strong-motion stations within 200 km of the epicenter, using the seismic moment and focal mechanism derived from long-period body-wave modeling. These seismograms are compared with the recorded seismograms in Figures 11 through 14, with all seismograms shown at their absolute times and scaled to their peak values which are indicated by arrows. At a distance of 100 km, the arrivals are, in order of increasing arrival time, the direct *S*, the Conrad refraction *Sc*, the Conrad reflection *ScS*, the Moho refraction *Sn*, and the Moho reflection *SmS*.

In the following, we examine the evolution of the recorded and synthetic seismograms with increasing distance from the source. At station SM16, at a distance of 43 km to the north, the direct *SV* wave is theoretically near a radiation pattern maximum. The fact that the recorded motion is not as large as the synthetic motion suggests incoherence in the radiation pattern. At station SM17, at a distance of 64 km to the west, the direct *SV* wave is theoretically near a radiation pattern

node, and its synthetic amplitude is less than that of the S to P free surface diffraction. The motions recorded at stations SM16 and SM17 suggest that reflected phases from the Conrad discontinuity are also present at these ranges. The arrival at SM16 (to the north) is slower than the model, while the arrival at SM17 (to the west) is faster. The other strong-motion recording stations within 200 km lie in the southwest quadrant and have arrival times that are in better agreement with the velocity model derived mainly from recordings in that quadrant.

At 90 km, the direct arrival has very small amplitude on both the recorded and synthetic seismograms. The largest phase in the recorded data at this distance is the postcritical reflection from the Conrad discontinuity; this phase is also present in the tangential component of the synthetic seismograms. However, both components of the synthetic seismograms also have large reflections from the Moho which are not apparent in the data, suggesting some inaccuracy in the structure model. Between 110 and 120 km, the recorded seismograms show large postcritical reflections from both the Conrad and the Moho; these are also present in the synthetic seismograms, and both reflections contribute to the largest motions. Beyond 150 km, the Moho reflection is masked by the Conrad reflection, which controls peak amplitudes out to 200 km.

In summary, the recorded and synthetic profiles both demonstrate that, at distances beyond about 70 km, the direct shear-wave arrival ceases to control peak ground motion amplitudes; instead, peak amplitudes are controlled by postcritical reflections from the velocity gradients in the lower crust. The strength of these postcritical reflections, and the distance ranges over which they are dominant, are controlled by the focal depth and crustal structure. Thus crustal structure and focal depth control the amplitude of strong ground motion as a function of distance from the source.

Attenuation of Ground Motion Amplitudes with Distance

The peak velocities and accelerations of the profiles of recorded and synthetic seismograms of Figures 11 through 14 are compared in Figure 15. The most important feature of the observed peak motions is that their amplitudes do not decay significantly with distance inside 120 km. The peak amplitudes of the synthetic tangential seismograms show the same feature, being relatively uniform out to 120 km and then abruptly decreasing. In both the recorded and synthetic seismograms in Figures 11 through 14, we have shown that the peak amplitudes in this flat portion of the attenuation curve inside 120 km are due to large postcritical reflections from the Conrad and Moho discontinuities. These reflections become postcritical at close distances because of the depth of the source. Some of the variability displayed in the synthetic peak motion values, and presumably also present in the recorded data, is due to the radiation pattern of the source, since for a given distance the amplitude depends on the azimuth of the station from the source. Use of the theoretical radiation pattern in the synthetic seismograms appears to produce more azimuthal variability than is observed at high frequencies in the recorded seismograms at stations SM16 and SM17, as described above.

Analysis of Lg Magnitude

North *et al.* (1989) measured the m_{bLg} of the Saguenay earthquake at six ECTN stations and obtained an average value of 6.5. They noted that this value is substantially larger than the teleseismic m_b of 5.9. Comparison of recorded and synthetic short-period P-wave amplitudes (Figs. 6 and 7) shows that the source

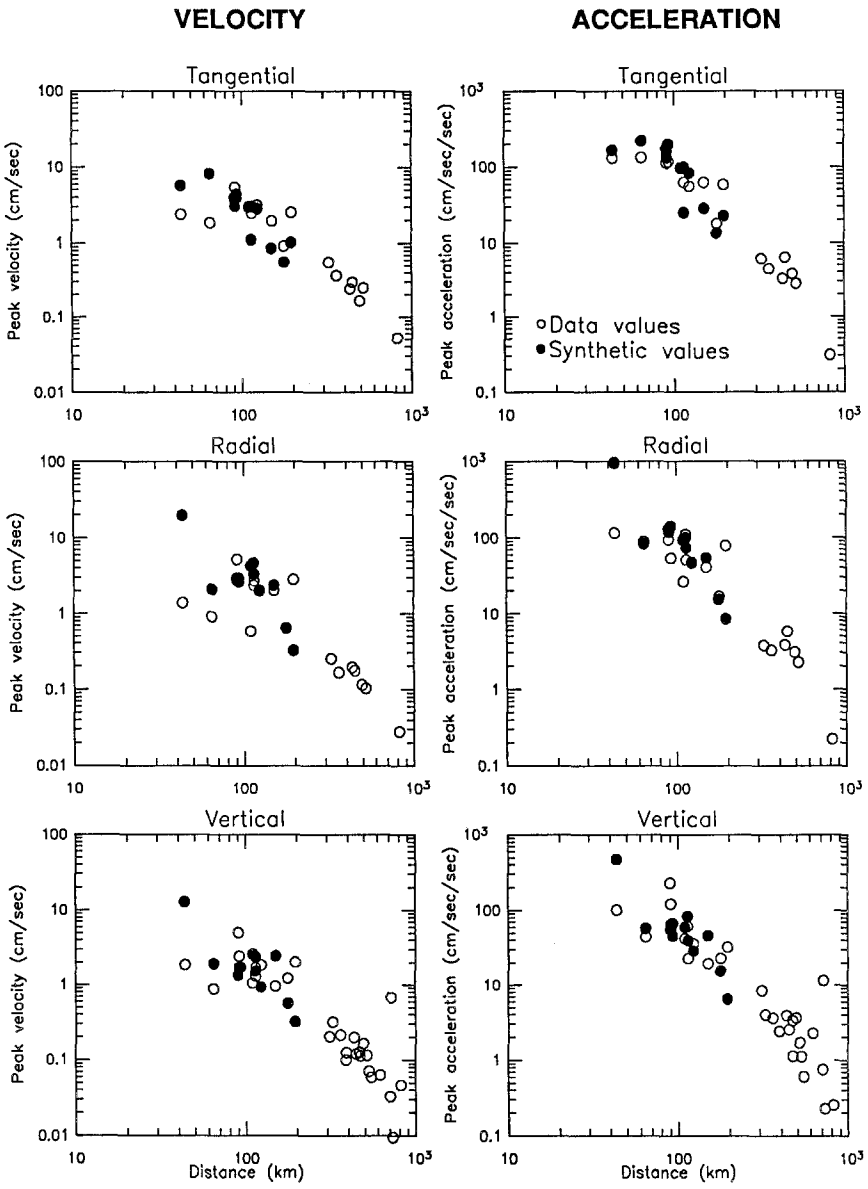

FIG. 15. Recorded (circles) and synthetic (dots) peak velocity (*left*) and peak acceleration (*right*) of the Saguenay earthquake as a function of epicentral distance.

model is compatible with the observed m_b of 5.9. We now wish to examine whether the source and regional wave propagation models that we have developed are consistent with the observed m_{bLg} of 6.5.

Using the source function shown in Figure 2, synthetic seismograms with a Nyquist frequency of 10 Hz were computed at seven ECTN stations in the distance range of 400 to 800 km in the Grenville province as an extension of the profile previously computed out to 200 km with a Nyquist frequency of 50 Hz to analyze the strong-motion recordings. The *Lg* portion of the synthetic seismograms (in the phase velocity range of 3.5 to 3.8 km/sec) was selected and Fourier transformed, and an attenuation operator derived from the Q model of Gariel and Jacob (1989)

was applied. The Q model has $Q = 110$ for frequencies less than 0.5 Hz, and $Q = 110 + 127\ (f - 0.5)$ for frequencies higher than 0.5 Hz, and was derived from analyses of recordings of the Saguenay earthquake in the Adirondacks and in Maine by Hough *et al.* (1989). The recorded *Lg* seismograms have considerably longer duration than the synthetic ones, particularly at frequencies higher than those that control *Lg* magnitude (above 1 to 2 Hz), suggesting that high frequency wave propagation, Q, and scattering are not well explained at these distances by the simple wave propagation model we have used.

Using the formula of Nuttli (1973), we obtained an average *Lg* magnitude of 6.42 for the seven Grenville Province ECTN stations (CKO, EEO, GRQ, JAQ, OTT, SZO, and WBO) from the synthetic seismograms, and 6.58 for the recorded seismograms; the latter value is in good agreement with the value of 6.5 measured by North *et al.* (1989) using a different set of stations. The discrepancy between the synthetic and recorded values is not considered to be significant in view of possible inaccuracies in the seismic velocity and Q models of the Grenville crust. We conclude that the source and regional wave propagation models developed in this study and the Q model of Gariel and Jacob (1989) are compatible with the observed *Lg* magnitude of the Saguenay earthquake.

The measured and synthetic m_{bLg} values exceed the value of 6.0 that is obtained from the seismic moment of the Saguenay event using an empirical relation between seismic moment and m_{bLg} for the larger historical eastern North American earthquakes. The empirical relation ($m_{bLg} = 0.59 \log M_o - 8.6$) is derived from the 12 eastern North American earthquakes listed in Table 1 of Somerville *et al.* (1987). Theoretical relations between M_o and m_{bLg} based on random process models (Boore and Atkinson, 1987; McGuire *et al.*, 1988) applied to the observed seismic moment give a similar m_{bLg} value of 6.1. We have found that the synthetic m_{bLg} value is not very sensitive to focal depth in our Saguenay crustal structure, but is sensitive to the Q model and to the spectral content of the source. The large m_{bLg} value of the Saguenay earthquake appears to be attributable in part to the peak in the source spectrum between 2 and 3 Hz shown in Figure 2.

Discussion

The large set of strong-motion recordings of the Saguenay earthquake provides the clearest evidence yet available of the effect of crustal structure on the attenuation of strong ground motion. Previous studies of other eastern North American earthquakes also indicate the importance of this influence and suggest that regional variations in ground motion attenuation may accompany regional variations in crustal structure. One of these studies used strong-motion recordings from the 1982 Gaza, New Hampshire, earthquake and from aftershocks of the 1982 New Brunswick earthquake, as well as seismograms from the 1983 Ottawa, Canada, 1983 Goodnow, New York, and 1986 Northeast Ohio earthquakes recorded on the ECTN (Barker *et al.*, 1988, 1989). Another study used calibrated digital seismograms from regional seismic networks in Virginia, the Central Mississippi Valley, and Mississippi (Saikia *et al.*, 1989).

In all of these regions, there is evidence from the recorded ground motions and from synthetic seismograms that postcritical reflections from velocity gradients in the lower crust produce elevated ground motion amplitudes over a certain distance range. Generally, the amplitudes are at most two to three times higher than those that would be obtained by extrapolating the attenuation curve from precritical distances. The distances over which the amplitudes are elevated generally lie in the

overall range of 50 to 200 km, with the specific distance range depending on the focal depth of the earthquake and on the crustal structure.

We have used synthetic seismograms to examine the influence of the deep focal depth of the Saguenay earthquake on the recorded strong ground motions. Figure 16 compares the predicted peak accelerations (average of two horizontal components plotted against epicentral distance) at the strong-motion recording stations for the actual depth of 28 km with those predicted for depths of 7.5 and 15 km. As in Figure 15, there are azimuthal variations among stations that produce variations in radiation pattern amplitudes. For the shallower depths, the peak motions are smaller within 40 to 100 km of the source but are larger beyond 100 km. This is because the critical distances of the Conrad and Moho reflections lie beyond 100 km for the shallower depths but lie within 100 km for the 28 km focal depth of the Saguenay earthquake. These results suggest that the strong motions would have been smaller in Chicoutimi (at 46 km) but larger in Quebec City (at 150 km) had the focal depth been shallower.

When strong-motion data from different crustal structures or from earthquakes from different focal depths are combined into a single data set, the detailed characteristics of regional attenuation relations are smeared out. This leaves a data set having a broad scatter that is most reasonably fit using a smooth attenuation curve that is applicable to the estimation of ground motions across eastern North America. However, if it is desired to estimate ground motions at a specific site or within a given region, then estimates having a lower degree of uncertainty can be obtained by using an attenuation curve that reflects the focal depths and wave propagation characteristics of that region.

There is evidence that postcritical reflections from the lower crust also control peak ground motion amplitudes in at least some regions of the western United

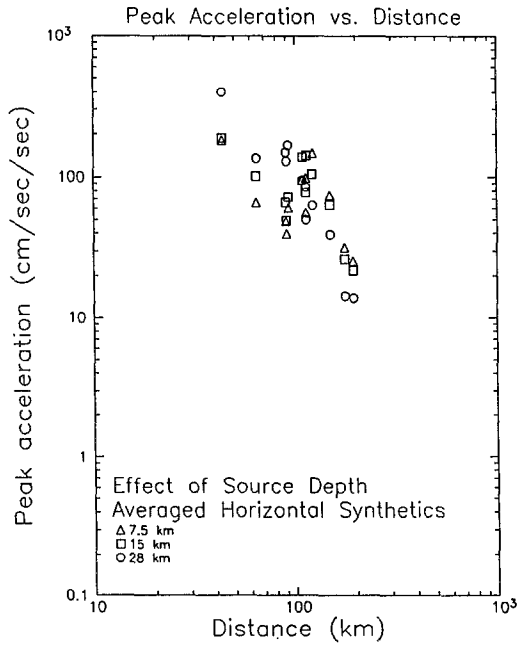

FIG. 16. Synthetic peak acceleration as a function of epicentral distance from the Saguenay earthquake for three focal depths.

States. Burger *et al.* (1987, Fig. 15) demonstrated that the largest ground motion velocities recorded at San Onofre (at a distance of 135 km) from the 1968 Borrego Mountain earthquake were due to postcritical reflections. Also, preliminary analysis of accelerograms having absolute times that were recorded during the 17 October 1989 Loma Prieta earthquake shows that in the distance range of 50 to 100 km (which includes San Francisco and Oakland), the largest motions at a given station were due to postcritical moho reflections (Somerville and Yoshimura, 1990). These motions were further amplified, presumably by impedance contrast effects, at soft soil sites. For both the Saguenay and Loma Prieta earthquakes, the short critical distance and the consequent elevation of ground motion amplitudes between about 50 and 120 km are due to deep focal depth, or more precisely, to the proximity of the source to the base of the lower crust.

Conclusions

The 25 November 1988 Saguenay earthquake is the largest earthquake to have occurred in a populated region of eastern North America since the magnitude 6.4 Timiskaming, Quebec, earthquake of 1935. It was caused by almost purely dip-slip faulting centered at a depth of 26 km with a P axis oriented northeast-southwest. The focal mechanism was similar to those of the larger earthquakes in the region, but the focal depth was substantially greater than all but one of these events (Ebel *et al.*, 1986; Somerville *et al.*, 1987). The seismic moment estimated from regional *Pnl* waves and long-period body waves was 5×10^{24} dyne-cm, corresponding to a moment magnitude of 5.8. The source duration of the earthquake was estimated to be 1.8 sec, corresponding to a stress drop of 160 bars. This stress drop was not significantly higher than the average stress drop of 120 bars estimated from the larger earthquakes in eastern North America by Somerville *et al.* (1987). In order to simultaneously match the recorded ground motion amplitude of strong-motion acceleration, strong motion velocity, and teleseismic short-period and long-period body waves, it was necessary to use a source function having a complex shape that implies the presence of asperities and larger local stress drops.

The Saguenay earthquake produced by far the largest set of strong motion recordings of any earthquake in eastern North America. The most important feature of these strong motions is that their amplitudes did not decay significantly with distance inside 120 km. The peak amplitudes of synthetic strong-motion seismograms showed the same lack of decay, being relatively uniform out to 120 km and then abruptly decreasing. In both the recorded and synthetic seismograms, the peak amplitudes inside 120 km were due to large postcritical reflections from the Conrad and Moho discontinuities. Because of the deep focal depth of the Saguenay earthquake, the critical distances for these reflections were short, causing the ground motion amplitudes to remain uniform out to 120 km. Modeling studies indicated that a shallower focal depth would have produced smaller ground motion amplitudes in the distance range of 43 to 100 km but larger ground motion amplitudes beyond 100 km as a result of the larger critical distance.

The strong-motion recordings of the Saguenay earthquake support a model for the attenuation of strong ground motion proposed by Burger *et al.* (1987) and investigated in several regions of eastern North America by Barker *et al.* (1988, 1989) and Saikia *et al.* (1989). According to this model, the shape of the attenuation curve within 200 km of the source is controlled by focal depth and crustal structure. Inside the critical distance for reflections from the lower crustal velocity gradient, peak ground motion amplitudes are controlled by upgoing shear waves. However,

beyond the critical distance, peak amplitudes are controlled by postcritical reflections from the velocity gradients in the lower crust. The strength of these postcritical reflections, and the distance ranges over which they are dominant, are controlled by the focal depth and crustal structure. Regional variations in crustal structure are therefore accompanied by regional variations in ground motion attenuation. Much of the scatter in empirical strong ground motion data in eastern North America may result from combining strong-motion data from different crustal structures or from earthquakes with different focal depths into a single data set, causing the detailed characteristics of regional attenuation relations to be obscured.

ACKNOWLEDGMENTS

We are grateful to many individuals in the Geological Survey of Canada for speedily providing data used in this study, including Mr. Robert Halliday, Mr. Philip Munro, Mr. William Shannon, and Ms. Anne Stevens. We also wish to acknowledge the strong-motion data provided by Dr. Klaus Jacob of Lamont-Doherty Geological Obervatory and seismograms provided by WWSSN seismograph station operators worldwide. Mrinal Sen participated in the initial modeling of the strong-motion records. The analysis of the Saguenay earthquake was sponsored by the Electric Power Research Institute under the direction of Drs. John Schneider and J. Carl Stepp.

REFERENCES

Barker, J. S., P. G. Somerville, and J. P. McLaren (1988). Modeling of ground-motion attenuation in eastern North America, Electric Power Research Institute Report NP-5577, 414 pp.

Barker, J. S., P. G. Somerville, and J. P. McLaren (1989). Modeling ground motion attenuation in eastern North America, *Tectonophysics* **167,** 139–149.

Berry, M. J. and K. Fuchs (1973). Crustal structure of the Superior and Grenville Provinces of the Northeastern Canadian Shield, *Bull. Seism. Soc. Am.* **63,** 1393–1432.

Boore, D. M. (1983). Stochastic simulation of high-frequency ground motions based on seismological models of the radiated spectra, *Bull. Seism. Soc. Am.* **73,** 1865–1984.

Boore, D. M. and G. M. Atkinson (1987). Stochastic prediction of ground motion and spectral response parameters at hard rock sites in Eastern North America, *Bull. Seism. Soc. Am.* **77,** 440–467.

Burger, R. W., P. G. Somerville, J. S. Barker, R. B. Herrmann, and D. V. Helmberger (1987). The effect of crustal structure on strong ground motion attenuation relations in eastern North America. *Bull. Seism. Soc. Am.* **77,** 420–439.

Cohn, S. N., T. L. Hong, and D. V. Helmberger (1982). The Oroville earthquakes: a study of source characteristics and site effects, *J. Geophys. Res.* **87,** 4585–4594.

Ebel, J. E., P. G. Somerville, and J. D. McIver (1986). A study of the source parameters of some large earthquakes in eastern North America, *J. Geophys. Res.* **91,** 8231–8247.

Friberg, P., R. Busby, D. Lentrichia, D. Johnson, K. Jacob, and D. Simpson 91989). The $M = 6$ Saguenay earthquake of November 25, 1988, near Chicoutimi, in the Province of Quebec, Canada: Preliminary Strong-Motion Data Report, in *The Saguenay earthquake of November 25, 1988, Quebec, Canada: strong motion data, ground failure observations, and preliminary interpretations*, K. H. Jacob (Editor). National Center for Earthquake Engineering Research.

Futterman, W. I. (1962). Dispersive body waves, *J. Geophys. Res.* **67,** 5279–5291.

Gariel, J.-C. and K. H. Jacob (1989). The Saguenay earthquake of November 25, 1988: the effect of the hypocentral depth on the peak acceleration: a modeling approach, in *The Saguenay earthquake of November 25, 1988, Quebec, Canada: strong motion data, ground failure observations, and preliminary interpretations*, K. H. Jacob (Editor). National Center for Earthquake Engineering Research.

Hanks, T. C. and R. K. McGuire (1981). The character of high-frequency strong ground motion, *Bull. Seism. Soc. Am.* **71,** 2071–2095.

Helmberger, D. V. and G. R. Engen (1980). Modeling the long-period body waves from shallow earthquakes at regional ranges, *Bull. Seism. Soc. Am.* **70,** 1699–1714.

Hough, S. E. and J. G. Anderson (1988). High-frequency spectra observed at Anza, California: implications for Q structure, *Bull. Seism. Soc. Am.* **78,** 692–707.

Hough, S. E., K. Jacob, and P. Friberg (1989). The 11/25/88, $M = 6$ Saguenay earthquake near Chicoutimi, Quebec: evidence for anisotropic wave propagation in northeastern North America, *Geophys. Res. Lett.* **16,** 645–648.

Langston, C. A. and D. V. Helmberger (1975). A procedure for modeling shallow dislocation sources, *Geophys. J. Roy. Astr. Soc.* **42,** 117–130.

McGuire, R. K., G. R. Toro, and W. J. Silva (1988). Engineering model of earthquake ground motion, Electric Power Research Institute Report NP 6074.

Munro, P. S., R. J. Halliday, W. E. Shannon, and D. R. J. Schieman (1988). *Canadian Seismograph Operations—1986. Geological Survey of Canada Paper 88-16*, Seismological Series Number 98.

Munro, P. S. and R. G. North (1988). The Saguenay earthquake of November 25, 1988: strong motion data. *Geological Survey of Canada Open-File Rept. 1976.*

North, R. G., R. J. Wetmiller, J. Adams, F. M. Anglin, H. S. Hasegawa, M. Lamontagne, R. Du Berger, L. Seeber, and J. Armbruster (1989). Preliminary results from the November 25, 1988 Saguenay (Quebec) earthquake, *Seism. Res. Lett.* **60,** 89–93.

Nuttli, O. W. (1973). Seismic wave attenuation and magnitude relations for eastern North America, *J. Geophys. Res.* **78,** 876–885.

Ou, G.-B. and R. B. Herrmann (1990). A statistical model for peak ground motion from local to regional distances, *Bull. Seism. Soc. Am.* (in press).

Saikia, C. K., P. G. Somerville, D. V. Helmberger, M. K. Sen, J. P. McLaren, L. J. Burdick, and N. F. Smith (1989). Ground-motion attenuation and earthquake source scaling in eastern North America, Electric Power Research Institute, Draft Report, 307 pp.

Somerville, P. G. (1986). Source scaling relations of eastern North American earthquakes, Electric Power Research Institute Report NP-4789, Palo Alto, California, 189 pp.

Somerville, P. G., J. P. McLaren, L. V. LeFevre, R. W. Burger, and D. V. Helmberger (1987). Comparison of source scaling relations of eastern and western North American earthquakes, *Bull. Seism. Soc. Am.* **77,** 332–346.

Somerville, P. G. and J. Yoshimura (1990). The influence of critical Moho reflections on strong ground motions recorded in San Francisco and Oakland during the 1989 Loma Prieta earthquake, *Geophys. Res. Lett.* **17,** 1203–1206.

Toro, G. R. and R. K. McGuire (1987). An investigation into earthquake ground motion characteristics in eastern North America, *Bull. Seism. Soc. Am.* **77,** 468–489.

Zhao, L.-S. and D. V. Helmberger (1989). Broadband modeling of the Quebec earthquake at regional distances, *EOS* **70,** 1228.

WOODWARD-CLYDE CONSULTANTS
566 EL DORADO STREET
PASADENA, CALIFORNIA 91101
(P.G.S., J.P.M., C.K.S.)

SEISMOLOGICAL LABORATORY
CALIFORNIA INSTITUTE OF TECHNOLOGY
PASADENA, CALIFORNIA
(D.V.H.)

Manuscript received 12 February 1990